Common Pool Resource Games with Network-Based Information Sets

Nicolas Schrama[1], Andrew Tilman[2], and Vítor V. Vasconcelos[1,3]

[1]Computational Science Lab, Informatics Institute, University of Amsterdam, Netherlands
[2]USDA Forest Service, Northern Research Station, United States of America
[3]POLDER, Institute for Advanced Study, University of Amsterdam, Netherlands

01-04-2023

Abstract

To come to a complete comprehension of common pool resource dynamics, we must first understand the information flows that drive users' incentives. This paper advances an agent-based model with boundedly rational common pool resource agents and information flows based on Barabasi-Albert networks. In the model, heterogeneity in the number of connections creates bistable resource equilibria, leading to an abundant and a scarce outcome. This result is driven by highly-connected users' influence on others' perceived network states. Allocating greater environmental weight to highly-connected individuals aligns their environmental impact and visibility, diminishing the difference between the abundant and scarce resource outcomes. These outcomes unite at the full-information equilibrium when highly-connected users are distributed sufficient environmental weight. Policymakers can leverage these findings regarding information asymmetries and the substantial influence of hub users to develop more informed approaches to CPR management in contexts such as food security and climate regulation.

1 Introduction

Common pool resources (CPRs)—encompassing critical environmental assets such as fisheries, forests, and the atmosphere—are foundational to both ecological sustainability and human societies. Their management and preservation are paramount, as they directly impact global food security, biodiversity, and climate regulation. CPRs are unique in their dual characteristics of non-excludability and resource depletion upon use, presenting intricate challenges in sustainable management [1]. Non-excludability implies challenges in restricting access to the resource, often leading to overuse and degradation, while subtractability means that one individual's use of the resource reduces its availability for others. These unique characteristics create complex resource management challenges, as traditional market mechanisms frequently fail to prevent overexploitation [1, 2]. Historically, managing these resources has been a complex issue, often leading to scenarios described by Hardin as "the tragedy of the commons" [3]. This concept illustrates how individual users, acting independently and rationally according to their self-interest, can ultimately deplete a shared resource to the detriment of the entire group's long-term best interests. This phenomenon is not just a theoretical construct but is evidenced in numerous real-world scenarios, such as overfishing in international waters and

deforestation in the Amazon basin [4]. In the contemporary context, the challenges posed by over-exploitation and mismanagement of CPRs have become even more pronounced due to factors like increased global demand, technological advancements in resource extraction, and climate change impacts. These challenges are further complicated by the intricate interplay of ecological dynamics and human behavior [5], making the sustainable management of CPRs a critical area of study in the realm of environmental science and policy [6].

The impacts of human activities on CPRs are extensive and complex. Driven by short-term benefits, unsustainable practices result in long-term ecological imbalances and resource scarcity. These effects have cascading implications for climate change, biodiversity, and human health. Studies emphasize that systems linking people and nature, known as social-ecological systems, are complex adaptive systems [7]. Their dynamics, including nonlinear feedbacks, strategic interactions, and heterogeneity, pose significant challenges for effective modeling and policy-making. Ignoring these complexities can lead to ineffective or counterproductive policies [7, 8].

Therefore, effective management and policy interventions must account for the intricate interplay between ecological systems and behavioral and socio-economic factors. They need to address the diverse interests, perspectives, and reach of stakeholders and strive for equitable and sustainable resource utilization [9].

Seminal works in CPR management have laid the foundation for understanding the complex dynamics of these systems. For instance, Ostrom's principles of collective resource management have been instrumental in illustrating how local communities can successfully manage CPRs through collective action and self-governance [1]. Her framework highlighted the importance of rules tailored to specific places and situations, local decision-making, monitoring, and graduated sanctions, among other factors, in effectively managing CPRs.

Recent advancements in the field have focused on the coevolution of behavior and resource dynamics, demonstrating how changes in human behavior can directly affect resource conditions and vice versa. Studies have shown that adaptive management strategies, where policies and practices evolve in response to changes in the system, can be more effective in dealing with the complexities of CPRs [10].

Building on [5], Tilman et al. [11] study the evolutional viability of a forecasting agent type, taking the middle road between rationality and myopia. They find that forecasting fosters collective intelligence by providing a public good which reduces the amplitude of environmental oscillations and often increases mean payoffs to forecasting and myopic types alike. Barfuss et al. [12] find that how much actors care for the future can transform the game from a tragedy of the commons into one of coordination.

This coevolution perspective underscores the dynamic interplay between human actors and the natural environment, which is central to understanding and managing CPRs sustainably.

Despite these advancements, significant gaps remain in the literature, particularly regarding the role of information asymmetry and social network structures in CPR management. While some studies have highlighted the importance of social networks in resource governance, the specific influence of highly visible or hub agents within these networks is less understood. Bodin and Crona's review shows structural properties like density and cohesiveness can impact governance processes [13]. Wilson et al., in the context of the Maine lobster fishery, demonstrate how competitive behaviors among fishers lead to the emergence of group structures that facilitate collective action for conservation [14]. Isaac et al. delve into the dynamics of informal advice networks in Ghanaian cocoa agroforestry systems, revealing how core farmers, often with access to external information, serve as vital conduits for the transfer of knowledge and practices within communities [15]. These studies provide valuable case-specific empirical observations into the relation between structural aspects of social networks and resource management. Generalizability to other contexts requires focusing on the information flow mechanisms and how these directly impact CPR sustainability.

This gap is particularly relevant in the context of modern environmental challenges, where the actions of a few key players or institutions can disproportionately affect the sustainability of resources. Understanding the influence of these hub agents and the asymmetry of information within social networks is therefore critical for developing effective management strategies and policies for CPRs.

While current literature acknowledges the complexity of social-ecological systems, particularly in the context of feedback dynamics between behavior and resource availability [5, 7, 11], it often overlooks the nuanced impact of information and overall player asymmetry in these networks. Specifically, the influence of hubs in shaping the perception and consequent actions of other agents in CPR scenarios remains underexplored. This poses significant limits to the broader understanding of CPR management, particularly how strategic behaviors and perceptions among CPR users are shaped through these networks.

This paper aims to bridge this gap by examining how information access and strategic behavior among CPR users are influenced through social networks, particularly focusing on the role and impact of hubs or highly visible agents.

Utilizing a game-theoretical agent-based model, this study investigates how agents' weight and extraction decisions, influenced by their social ties, co-evolve with and impact the sustainability of common pool resources. We explore the cognitive parameters and information limitations within these networks, thereby providing a nuanced understanding of CPR management under varying conditions of bounded rationality.

The model simulates the decision of indivual agents in a population of CPR users. Agents choose between extracting from the resource with low effort or high effort, thereby influencing the evolution of the resource state. Their decision depends on the resource state they perceive and their expectations of other users' behavior. The resource state in the model is normalized between 0 and 1. Differences in agents' (number of) social ties generate heterogeneous information and visibility. Recognizing that highly visible players plausibily exert concomitant environmental impact, we consider an inequality of environmental impact parameter that amplifies the environmental impact of agents with many social ties.

The study reveals that network structures, particularly skewed degree distributions, lead to multiple possible CPR outcomes corresponding to alternative stable states for the same external conditions. A key finding is the substantial influence of hub agents in shaping network perceptions and decisions, creating phenomena like majority illusions that significantly affect resource states and sustainability. As inequality of impacts rises, this effect disappears, but access to a state with higher welfare also disappears. These findings highlight the critical role of network hubs in CPR dynamics, offering new directions for effective management and policy-making.

The remainder of the paper starts with Section 2, which presents the simulations results. Section 3 provides a discusssion of the results in the context of the literature and offers future research directions. Supplemental materials include parameter details, an outline of the model, and global sensitivity analysis.

2 Results

2.1 A majority illusion creates bistable resource outcomes

The model can simulate diverse common pool resource scenarios that differ in terms of environmental dynamics, user incentives, and social network structure. In this paper, we study a common pool resource with two crucial characteristics.

First, we consider incentives for individuals to act against the majority (choosing high effort when others choose low effort and vice versa). These incentives are reflected by the relationship between

U_t^d - the utility advantage of extracting with high effort relative to low effort - and expectations regarding the fraction of users extracting with low effort z_t^e, given by Equation 1.

$$\begin{aligned} \frac{\mathrm{d}U_t^d}{\mathrm{d}z_t^e} &= \gamma_1^H - \gamma_1^L + \gamma_3^H - \gamma_3^L \\ &= \gamma_1^d + \gamma_3^d \end{aligned} \tag{1}$$

When the derivative in Equation 1 is positive, extracting with high effort becomes more advantageous as z_t^e increases. Since z_t represents the fraction of agents extracting with low effort, positive values of γ_1^d and γ_3^d encourage coordination while negative values discourage it. Global sensitivity analysis (see the Method details for the complete results) underscores the substantial impact of these incentives on the model's outcomes.

In the context of this paper, where $\gamma_2^d < 0$ and $\gamma_3^d = 0$, incentives against coordination exist. Ecologically, these incentives reflect users who exhibit opportunistic behavior (choosing high effort when others opt for low effort) yet demonstrate an aversion to resource depletion (preferring low effort when others engage in high effort).

The concept of coordination incentives is closely related to expectations feedback in the learning to forecast literature [16, 17, 18]. Research in this domain highlights that incentives to act against the majority lead to stable dynamics that tend to the full-information equilibrium (FIE). Conversely, incentives favoring alignment with the majority result in oscillating dynamics that fail to converge to the full-information equilibrium.

Second, social network structures are generated using the Barabasi-Albert algorithm, resulting in scale-free networks with a skewed degree distribution. According to the global sensitivity analysis, the number of links in the network significantly impacts the model outcomes.

We simulate the model with 1000 agents over 40,000 periods. The Key Resource Table provides the complete set of parameters. The results of 100 simulations of the model are illustrated in Figure 1. Each blue curve represents the state of the common pool resource over time for one simulation. The simulations differ only in their seed values. The dashed line indicates the full-information equilibrium. The simulation results reveal two equilibrium levels of the resource state: an abundant outcome and a scarce outcome. The resource state exhibits stability over time.

The panel on the right side of Figure 1 shows the frequency of the two outcomes, demonstrating a 25—75 split, with about 25% of the simulations resulting in a resource level below the full-information equilibrium. These findings prompt two questions: why do two possible resource outcomes arise, and what dynamics underlie deviations from the FIE?

We delve into the incentives agents face over time to answer these questions. Figure 2 illustrates the utility advantage U_t^d over time in a single simulation featuring an abundant resource state. Each dot in Figure 2 corresponds to a single agent in a single period. The color of the dot indicates the agent's degree. Agents displayed in yellow have many social ties, while the agents displayed in dark purple have few social ties. The histogram in the panel on the right illustrates the final distribution of the utility advantages. The colors of the bars indicate the average degree of agents associated with the respective (binned) utility advantages. The frequencies in the bar plot are derived from the last 10,000 time points over 100 simulations.

Figure 2 demonstrates a vertical ordering of degrees, indicating that the network's most connected agents perceive the highest utility advantages, while the least connected agents perceive the lowest utility advantages. This ordering is depicted by the dots in the left panel and the bars in the right panel.

Highly-connected agents, perceiving exclusively positive utility advantages, consistently opt for high-effort extraction. The visibility of these agents creates the perception among most users that the average extraction level in the population is high. Social scientists refer to the phenomenon where

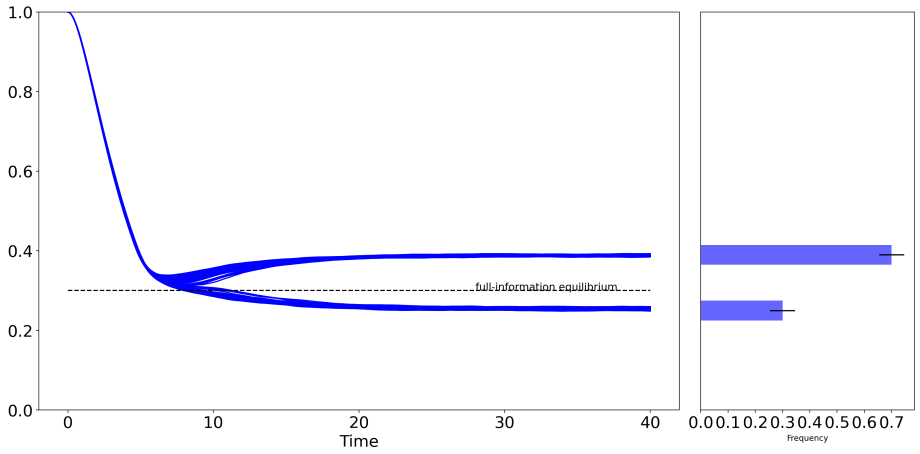

Figure 1: Infomation asymmetry generates two alternative equilibrium levels of resource outcomes. Each blue line represents the resource level over time for a single simulation on a heterogeneous network. The right panel shows the distribution of the model outcomes. There is a 25-75 split of the simulations, with about 25% resulting in a stable resource level below the full-information equilibrium, FIE (dashed lined), and 75% above. The social network, a Barabasi-Albert network with scale-free distribution of links, defines the differences in how much information agents obtain and which information they obtain. Agents that obtain more information are also more visible to the rest of the population. In this setup, the model's incentive structure encourages agents to go against the majority. This plot shows the results of 100 simulations of the model that differ only in seed.

globally rare network states are overrepresented in the local neighborhoods of many individuals as the majority illusion. Due to incentives to act against the majority, the predominant share of the population chooses low-effort extraction. Consequently, the realized population-level extraction is low, resulting in an abundant resource state. Thus, in systems with incentives to oppose the majority, beneficial resource outcomes emerge when highly visible users extract from the resource extensively, thereby incentivizing others to sustain it.

Figure 3 illustrates the utility advantage over time in a single simulation featuring a scarce resource state. Compared to Figure 2, the vertical ordering of users' degrees in Figure 3 is inverted, as the most connected users now observe the lowest utility advantages. The figure illustrates that scarce resource states emerge when the network's most connected users opt for low-effort extraction, creating a perception of low population-level extraction. Consequently, users with few connections are incentivized to engage in high-effort extraction, resulting in a scarce resource outcome.

Figures 2 and 3 highlight a relationship between users' states and their degrees. When high-degree users extract with high effort - a positive correlation between state and degree - the abundant outcome emerges, while a negative correlation leads to a scarce outcome. This correlation arises when the utility advantage reaches zero, and the first users start to extract with low effort. The sign of the correlation settles randomly within a few generations after its manifestation and persists throughout the simulation. Thus, the state-degree correlation and its stochastic emergence elucidate the bistability observed in the model's equilibria.

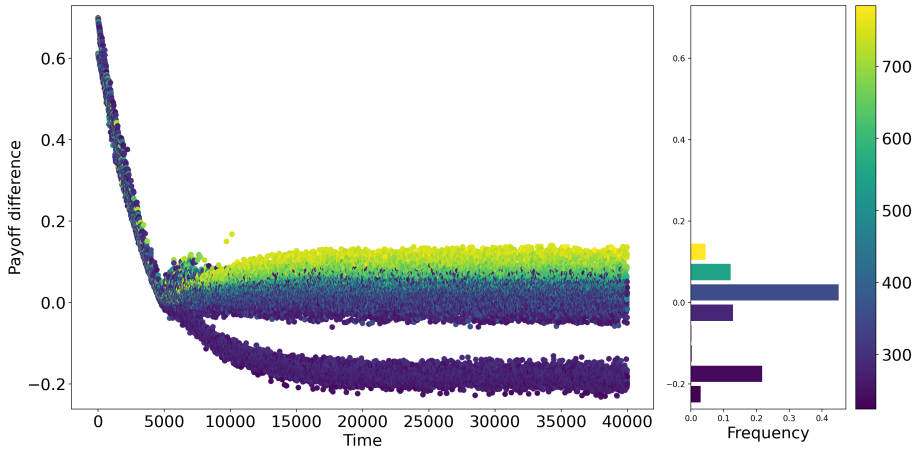

Figure 2: Distribution of the utility advantange of high-effort extraction relative to low-effort extraction in a single typical abundant resource state simulation. Each dot corresponds to a single agent in a single simulation round. The color of the dot represents that agent's degree. The histogram on the right side provides the final distribution of the utility advantages. The colors of the bars represent the average degree of the agents that perceived these (binned) utility advantages. The frequencies in the bar plot are based on the last 10000 time points over 100 simulations. In Barabasi-Albert networks, a few agents possess most of the connections. The abundant outcome occurs when the network's most connected agents extract with high effort. The visibility of these agents creates the perception among most agents that the average extraction level in the population is high. Social scientists refer to the phenomenon where globally rare network states that are overrepresented in the local neighborhoods of many individuals as the majority illusion. As a result of incentives to go against the majority, the predominant share of the population that has few connections extracts with low effort. Consequently, the realized population-level extraction is low, leading to an abundant resource state.

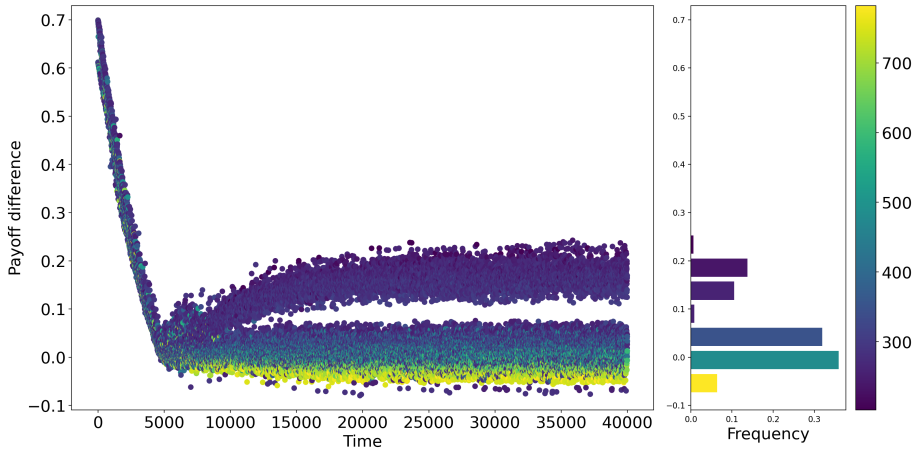

Figure 3: A scarce resource state emerges when the network's most connected agents extract with low effort, which occurs in this case because most connected agents percieve a negative payoff advantage to high effort extraction. This creates a perception among a majority of agents of low population-level extraction. This perception results in an incentive to extract with high effort among agents with few connections and, in turn, a scarce resource outcome. In other words, a relation exists between state and degree. When high-degree agents extract with high effort, i.e., a positive correlation between state and degree, the abundant outcome emerges, while a negative correlation leads to a scarce outcome. This correlation arises when the utility advantage reaches zero, and the first users start to extract with low effort. The sign of the correlation settles randomly within a few generations after its manifestation and persists throughout the simulation. Thus, the state-degree correlation and its stochastic emergence explain the bistability in the model's steady states.

2.2 The skewness of the degree distribution determines the difference between the stable resource state

Section 2.1 discussed the emergence of bistability in the model's outcomes and its underlying dynamics. This section highlights the structure of the social network, in particular the skewness of the degree distribution, as a critical factor determining the size of the difference between the two stable outcomes.

Figure 4 displays resource state outcomes across various skewness levels of the degree distribution. Each dot denotes the average resource state in the last hundred periods of a simulation, with 30 simulations plotted per skewness level. The dashed horizontal line represents the FIE, while the solid vertical line corresponds to the skewness level of the degree distribution in Figures 1, 2, and 3. Figure 4 illustrates the emergence and persistence of bistability in resource state outcomes as the skewness of the degree distribution increases.

The skewness of the degree distribution results from the initialization of the Barabasi-Albert algorithm, which operates by sequentially adding new nodes and connecting them to existing ones. The algorithm's parameters are the number of nodes at termination (P) and the number of existing nodes to which a new node is connected (λ). For example, if the network terminates with 1000 nodes and new nodes connect to 950 existing nodes, the network initializes with 950 nodes that each have no edges. Then, 50 nodes are sequentially added each linking to 950 existing nodes, becoming hubs. The initial 950 nodes obtain approximately 48-50 connections each. In this case, a high value of λ yields a significantly skewed degree distribution.

Relative to degree distributions with minimal skew, degree distributions with substantial skew exhibit two significant characteristics: (i) the central part of the degree distribution vanishes while

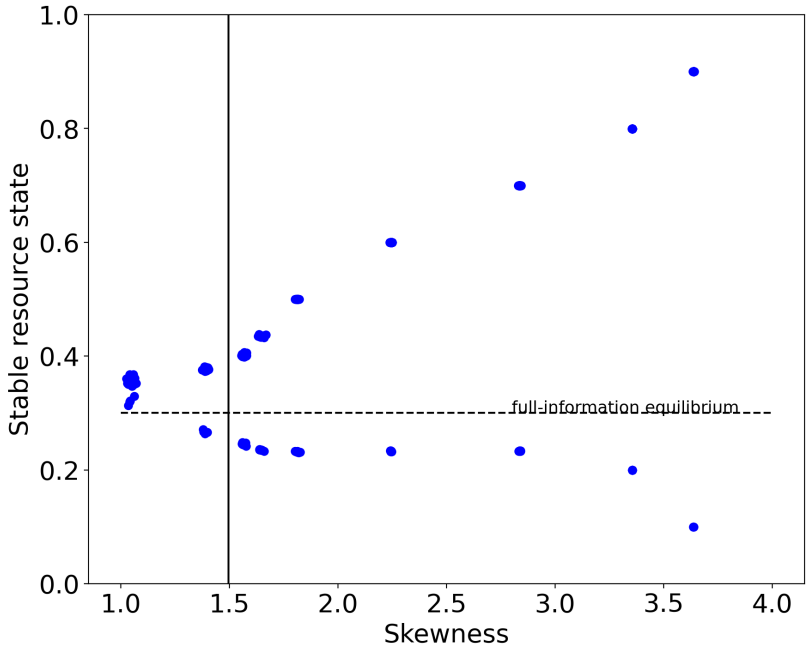

Figure 4: Spread of the model outcomes increases as the skewness of the degree distribution increases. This skewness results from the initialization of the BA algorithm. For example, if the network has a 1000 nodes and 950 nodes are added for each new node, the network is initialized with 950 nodes that each have no edges. Then, 50 nodes are added sequentially with 950 connections each. These become the hubs. The other 950 nodes end up with about 48-50 connections. This results in a mega-skewed degree distribution. On the horizontal axis of the plot is the skewness of the degree distribution, and on the vertical axis is the model's steady state. Each dot corresponds to the average resource state in the last hundred time points of a simulation. The plot is based on 30 simulations per link density. The plot shows the emergence and persistence of bistability in the model as the skewness increases. The difference between the steady states for a given link density increases as the skewness increases. As the degree distribution becomes more skewed, two things occur: (i) the middle of the degree distribution disappears while the number of low-degree agents increases, and (ii) the degrees of most agents decrease. Consequently, the low-degree agents' perception of population extraction levels becomes more skewed towards the hubs. Incentives to go against the majority drive this majority of agents to choose high effort when the hubs choose low effort and vice versa. Because of the increasing size of this group, the difference between the two steady states increases.

the number of low-degree nodes increases, and (ii) most users' degree decreases. Consequently, the population of low-degree users expands and low-degree users' perception of population extraction levels becomes increasingly biased towards the hubs. Incentives against coordination compell an increasingly large fraction of users to choose high effort when the hubs choose low effort and vice versa. These dynamics translate to an increasing difference between the model's steady states as the skewness of the degree distribution increases.

2.3 Inequality of environmental impact mitigates the majority illusion

Section 2.2 demonstrated that the heightened visibility of hubs in significantly skewed degree distributions results in a more pronounced difference between the model's two stable resource outcomes. Common pool resource users with substantial visibility plausibly exert concomitant environmental impact. To address this relationship, we introduce an inequality of environmental impact parameter (ν) that allocates a greater environmental weight to highly-connected individuals.

A user's environmental impact is determined by an exponential relation between the network degree and the inequality of environmental impact. As inequality of impact increases, the evolution of the resource state becomes increaslingly dependent on high-degree users and less on low-degree users. Environmental impact is homogeneous when the inequality of environmental impact parameter equals zero, as in Figures 1, 2, 3, and 4.

Figure 5 displays resource state outcomes across various levels of inequality of environmental impact. Each dot denotes the average resource state in the last hundred periods of a simulation, with 30 simulations plotted per value of the inequality of environmental impact parameter. The dashed horizontal line indicates the FIE.

Figure 5 illustrates the diminishing difference between the model's two steady states as inequality of environmental impact increases, culminating in the subsidence of bistability when inequality of environmental impact reaches a critical value. The single remaining steady state equals the FIE.

The deviations from the FIE in Figure 4 stem from the overrepresentation of high-degree users' behavior in the local neighborhoods of many users, creating a majority illusion. As the inequality of environmental impact increases, users' perceptions of the population extraction level become more in line with the true extraction level. This alignment occurs because hubs are not only overrepresented in terms of visibility but also in terms of environmental impact. Consequently, low-degree users' information becomes more accurate as the inequality of environmental impact increases, guiding the model outcome towards the FIE.

Thus, bistability exists in the model when the inequality of environmental impact is below its critical value, whereas a single steady state exists at the FIE when the inequality of environmental impact is at or above its critical value.

3 Discussion

Common pool resource users operate in environments where the strategies of others are not always common knowledge. But if access to information is unequal, will individuals with more information be favored when making strategic decisions? We investigate the dynamics of social networks in the context of common pool resource management, highlighting the role of information asymmetries and strategic behavior, particularly among hub users. Key findings include the emergence of bistable CPR outcomes driven by skewed degree distributions, the significant impact of hub users on network perceptions and decisions, and the potential subsidence of a majority illusion due to the inequality of environmental impact. We demonstrate that network structure substantially impacts CPR dynamics, generating bistable equilibria. This bistability yields access to a high-welfare state with the risk of

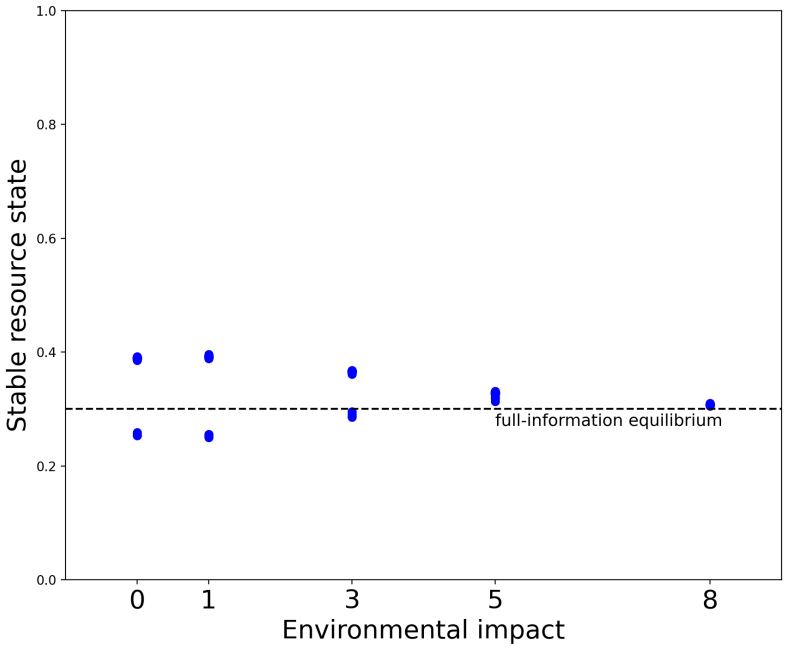

Figure 5: Bistability disappears with unequal impact distribution as high-degree nodes have an impact increasingly proportional to their degree. Here, we focus on how the distribution of the model outcomes changes as agents' environmental impact becomes increasingly related to their degrees. In the model, an agent's environmental impact depends on an exponential relation between the network degree and the environmental impact parameter. The parameter representing this relation is the inequality of impact. When the inequality of impact increases, the evolution of the resource state becomes more dependent on high-degree agents and less dependent on low-degree agents. On the horizontal axis is the inequality of environmental impact. On the vertical axis is the model's steady state. Each dot corresponds to the average resource state in the last hundred time points of a simulation. The Figure is based on 30 simulations per value of the environmental impact parameter. The plot shows the subsidence of bistability in the model as the inequality of environmental impact increases. Agents' environmental impact is homogeneous when the inequality of environmental impact parameter equals zero, as in Figure 1. As inequality of environmental impact increases, the difference between the model's two steady states decreases, leading to the subsidence of bistability when inequality of environmental impact reaches a critical value. This single steady state equals the FIE. The deviations from the FIE stem from the overrepresentation of high-degree agents' decisions in the local neighborhoods of many agents, creating a majority illusion. As inequality of environmental impact increases, agents' perception of the population extraction level becomes more in line with the true extraction level because high-degree are not only overrepresented in the local neighborhoods of low-degree agents but also in terms of their environmental impact. Consequently, low-degree agents' information becomes more accurate as inequality of environmental impact increases, steering the model outcome towards the FIE. Thus, bistability exists in the model when inequality of environmental impact is below its critical value, while there is a single steady state at the FIE when it's at or above its critical value.

ending up in a low-welfare state. The difference in resource state between these two outcomes depends on the balance between the visibility and environmental impact of hub users.

The present work finds a critical positioning in between fully tractable mathematical models and real-world case studies. Compared to the existing, fully-tractable models with dynamic environments and feedbacks between the environment and strategic behavior [5, 11, 12], the present study offers a more realistic behavioral model with heuristics-based decision-making and network-based information sets. Particularly the use of networks is impossible in the fully-tractable approach. In comparison to applied studies, such as [14, 15], the use of an agent-based model provides a systematic framework for exploring complex CPR management scenarios, user incentives, and social network structures. As a result, we can go beyond the observation that social networks exist among CPR users and come to a comprehensive explanation of how network structures impact CPR sustainability.

The study underscores the importance of considering social network dynamics and information asymmetries in designing effective CPR management policies. Insights into the disproportionate influence of hub agents and the potential mitigation of the majority illusion offer valuable avenues for policymakers to enhance resource governance strategies. The results suggest that managers should first investigate the system's incentives, the structure of the social network, and whther visibility and enviromental impact are aligned. When the rules of the game incentivize opportunistic (extracting substantial amounts when others are not) but depletion-averse behavior, managers can improve environmental outcomes simply by bringing to the public attention the extraction activities of users with substantial environmental influence but little visibility. Policymakers can leverage these findings to develop more adaptive and informed approaches to CPR management, fostering sustainability.

There really should be a real-world example here but I can't think of any.

To facilitate managers in comprehending the influence of social network structures on CPR outcomes and creating effective policies, we have developed a publicly available visual tool. By offering a user-friendly interface and customizable options, the tool empowers managers to analyze network structures, identify key influencers, and evaluate potential policy interventions. We invite managers and practitioners to use the tool, providing valuable feedback to enhance its functionality and relevance to real-world CPR management challenges.

Future research endeavors could explore the transferability of the study's findings to diverse common pool resource contexts, shedding light on the interaction between social network structures and case-specific factors. This undertaking holds significant potential for putting the study's results into practical use and informing policy in CPR management. By examining the applicability of the study's findings across different contexts, future research can contribute to the development of more contextually relevant and effective CPR management strategies.

Limitations

The model's abstraction oversimplifies the complexities of real-world CPR management, limiting insights into the interaction between hubs' influence on network perceptions and decisions with context-specific factors, such as socials norms, the spatial distribution of the resource, or local laws [19]. Abstraction also limits the model's immediate applicability to practical CPR management contexts, requiring greater initial effort to include context-specific factors. Furthermore, no policy interventions are explicitly modeled within the framework. To study the effects of potential policies, managers must formulate these policies in terms of the constructs present within the model.

Star Methods

Detailed methods are available online and include the following:

- *Key resource table*
- *Resource Availability*
  - Lead contact
  - Materials availability
  - Data and code availability
- *Method details*
  - Agent-based model
  - Global sensitivity analysis
  - System Rationality
  - Hartigan's dip test

Supplemental information

Supplemental information can be found online at **DOI**.

Acknowledgements

This work was supported by the USDA Forest Service (**grant number**).

Author contributions

All authors designed and performed the research as well as wrote the paper.

Declaration of interest

The authors declare no competing interests.

References

[1] E. Ostrom, *Governing the Commons: The Evolution of Institutions for Collective Action*. Political Economy of Institutions and Decisions, Cambridge University Press, 1990.

[2] T. Dietz, E. Ostrom, and P. C. Stern, "The struggle to govern the commons," *Science*, vol. 302, no. 5652, pp. 1907–1912, 2003.

[3] G. Hardin, "The Tragedy of the Commons," *Science*, vol. 162, no. 3859, pp. 1243–1248, 1968. Publisher: American Association for the Advancement of Science.

[4] D. Feeny, F. Berkes, B. Mccay, and J. Acheson, "The tragedy of the commons: Twenty-two years later," *Human Ecology*, vol. 18, pp. 1–19, 03 1990.

[5] A. R. Tilman, J. B. Plotkin, and E. Akçay, "Evolutionary games with environmental feedbacks," *Nature Communications*, vol. 11, p. 915, Feb. 2020. Number: 1, Publisher: Nature Publishing Group.

[6] A. Agrawal, "Common property institutions and sustainable governance of resources," *World Development*, vol. 29, no. 10, pp. 1649–1672, 2001.

[7] S. Levin, T. Xepapadeas, A.-S. Crépin, J. Norberg, A. d. Zeeuw, C. Folke, T. Hughes, K. Arrow, S. Barrett, G. Daily, P. Ehrlich, N. Kautsky, K.-G. Mäler, S. Polasky, M. Troell, J. R. Vincent, and B. Walker, "Social-ecological systems as complex adaptive systems: modeling and policy implications," *Environment and Development Economics*, vol. 18, pp. 111–132, Apr. 2013. Publisher: Cambridge University Press.

[8] F. Berkes, ed., *Common property resources: Ecology and community-based sustainable development*. London; New York: Belhaven Press, 1989 1989. Published in association with the International Union for Conservation of Nature and Natural Resources; Conference on Conservation Development Implementing the World Conservation Strategy (1986: Ottawa, Ont); World Congress of Ecology (4th: 1986: Syracuse, NY).

[9] E. Ostrom, "Coping with Tragedies of the Commons: Local Lessons, Global Challenges," jan 2000.

[10] F. Berkes and D. Jolly, "Adapting to climate change: Social-ecological resilience in a canadian western arctic community," *Conservation Ecology*, vol. 5, no. 2, 2002.

[11] A. R. Tilman, V. V. Vasconcelos, E. Akçay, and J. B. Plotkin, "The evolution of forecasting for decision-making in dynamic environments," *Collective Intelligence*, vol. 2, no. 4, p. 26339137231221726, 2023.

[12] W. Barfuss, J. F. Donges, V. V. Vasconcelos, J. Kurths, and S. A. Levin, "Caring for the future can turn tragedy into comedy for long-term collective action under risk of collapse," *Proceedings of the National Academy of Sciences*, vol. 117, no. 23, pp. 12915–12922, 2020.

[13] Bodin and B. I. Crona, "The role of social networks in natural resource governance: What relational patterns make a difference?," *Global Environmental Change*, vol. 19, pp. 366–374, Aug. 2009.

[14] J. Wilson, L. Yan, and C. Wilson, "The precursors of governance in the Maine lobster fishery," *Proceedings of the National Academy of Sciences of the United States of America*, vol. 104, pp. 15212–15217, Sept. 2007.

[15] M. Isaac, B. Erickson, S. Quashie-Sam, and V. Timmer, "Transfer of knowledge on agroforestry management practices: The structure of farmer advice networks," *Ecology and Society*, vol. 12, no. 2, 2007.

[16] C. Hommes, "Behavioral and experimental macroeconomics and policy analysis: A complex systems approach," *Journal of Economic Literature*, vol. 59, Mar. 2021.

[17] P. Heemeijer, C. Hommes, J. Sonnemans, and J. Tuinstra, "Price stability and volatility in markets with positive and negative expectations feedback: An experimental investigation," *Journal of Economic Dynamics and Control*, vol. 33, pp. 1052–1072, May 2009.

[18] T. Bao, C. H. Hommes, J. Sonnemans, and J. Tuinstra, "Individual expectations, limited rationality and aggregate outcomes," *Journal of Economic Dynamics & Control*, vol. 36, 2012.

[19] E. Ostrom, "A general framework for analyzing sustainability of social-ecological systems," *Science (New York, N.Y.)*, vol. 325, pp. 419–422, July 2009.

[20] V. Grimm, U. Berger, F. Bastiansen, S. Eliassen, V. Ginot, J. Giske, J. Goss-Custard, T. Grand, S. K. Heinz, G. Huse, A. Huth, J. U. Jepsen, C. Jørgensen, W. M. Mooij, B. Müller, G. Pe'er, C. Piou, S. F. Railsback, A. M. Robbins, M. M. Robbins, E. Rossmanith, N. Rüger, E. Strand,

S. Souissi, R. A. Stillman, R. Vabø, U. Visser, and D. L. DeAngelis, "A standard protocol for describing individual-based and agent-based models," *Ecological Modelling*, vol. 198, pp. 115–126, Sept. 2006.

[21] V. Grimm, U. Berger, D. L. DeAngelis, J. G. Polhill, J. Giske, and S. F. Railsback, "The ODD protocol: A review and first update," *Ecological Modelling*, vol. 221, pp. 2760–2768, Nov. 2010.

[22] V. Grimm, S. F. Railsback, C. E. Vincenot, U. Berger, C. Gallagher, D. L. DeAngelis, B. Edmonds, J. Ge, J. Giske, J. Groeneveld, A. S. A. Johnston, A. Milles, J. Nabe-Nielsen, J. G. Polhill, V. Radchuk, M.-S. Rohwäder, R. A. Stillman, J. C. Thiele, and D. Ayllón, "The ODD Protocol for Describing Agent-Based and Other Simulation Models: A Second Update to Improve Clarity, Replication, and Structural Realism," *Journal of Artificial Societies and Social Simulation*, vol. 23, no. 2, p. 7, 2020.

[23] M. Anufriev and C. Hommes, "Evolutionary selection of individual expectations and aggregate outcomes in asset pricing experiments," 2011. Publisher: AmsterdamUniversiteit van Amsterdam.

[24] I. M. Sobol, "Global sensitivity indices for nonlinear mathematical models and their Monte Carlo estimates," *Mathematics and Computers in Simulation (MATCOM)*, vol. 55, no. 1, pp. 271–280, 2001. Publisher: Elsevier.

[25] A. Saltelli, "Making best use of model evaluations to compute sensitivity indices," *Computer Physics Communications*, vol. 145, pp. 280–297, May 2002.

[26] A. Saltelli, P. Annoni, I. Azzini, F. Campolongo, M. Ratto, and S. Tarantola, "Variance based sensitivity analysis of model output. Design and estimator for the total sensitivity index," *Computer Physics Communications*, vol. 181, pp. 259–270, Feb. 2010.

[27] D. Kasthurirathna and M. Piraveenan, "Emergence of scale-free characteristics in socio-ecological systems with bounded rationality," *Scientific Reports*, vol. 5, p. 10448, June 2015. Number: 1 Publisher: Nature Publishing Group.

[28] Thomas M. Cover and Joy A. Thomas, "Entropy, relative entropy and mutual information," no. 2(1), pp. 12–13, 1991.

[29] J. Lin, "Divergence measures based on the Shannon entropy," *IEEE Transactions on Information Theory*, vol. 37, pp. 145–151, Jan. 1991. Conference Name: IEEE Transactions on Information Theory.

[30] J. A. Hartigan and P. M. Hartigan, "The dip test of unimodality," *The Annals of Statistics*, vol. 13, no. 1, pp. 70–84, 1985.

Star Methods

Key Resource Table

The parameter values used in the simulations are provided by Table 1.

Resource availability

Lead contact

Further information and requests for resources should be directed to and will be fulfilled by the Lead contact Nicolas Schrama (npn98@hotmail.nl).

Table 1: Parameter configuration of the model.

Parameter	Value	Description
α	-0.3	Payoff difference between extracting with high and low effort in an extracted environment
γ_1^L	0.5	Linear relation of the average action other of users in the low-effort payoff
γ_2^L	1.5	Linear relation of the environment in the low-effort payoff
γ_3^L	0	Nonlinearity of low-effort payoff surface
γ_1^H	0.75	Linear relation of the average action of other users in the high-effort payoff
γ_2^H	2.25	Linear relation of the environment in the high-effort payoff
γ_3^H	0	Nonlinearity of high-effort payoff surface
ϵ	0.25	Relative speed of environmental and strategic dynamics
P	1000	Number of agents
σ	0.1	Slope of sigmoid
β_1	0.63	Coefficient adaptive expectations
β_2	0.44	Coefficient trend-chasing expectations
β_3	-0.44	Coefficient contrarian expectations
ρ	0.9	Probability to update heuristic
η	0.7	Memory of prior heuristic utility
ϕ	100	Choice intensity
λ	250	Link density in the Barabasi-Albert algorithm
ν	0	Inequality of environmental impact

Table 2: State variables of the model.

Entity	State Variable	Relevance
Agent	Memory ledger	Tracks other agents' strategic decisions, used for observation and resource state perception updating
	Observations	Snapshots of population-wide extraction levels used to form expectations about future extraction levels
	Resource state perception	Used for choosing a strategy
	Heuristic	Rule used for expectation formation
Environment	Resource state	Model output of interest

Materials availability

We have developed a publicly available visual tool to facilitate managers in comprehending the influence of social network structures on CPR outcomes and creating effective policies. It is available at github, doi.

Data and code availability

No data was used to generate the results in this paper. The code used to generate the figures is available online **github, doi**.

Method details

Agent-based model

A complete, detailed model description, following the ODD (Overview, Design concepts, Details) protocol [20, 21, 22] is provided at **Insert link to web repository where you uploaded your ODD**.

This paper aims to study the role of information access on strategic behaviors of common pool resource users through social networks. Agents choose between extracting from the resource with low effort or high effort, thereby influencing the evolution of the resource state. Differences in agents' number of social ties generate heterogeneous visibility. The purpose of the model is to create a framework through which the impact of the behavior of highly visible agents on the rest of the population can be analyzed. Recognizing that highly visible players can potentially have a large environmental impact, we consider an inequality of environmental impact parameter that amplifies the environmental impact of agents with many social ties.

The model includes the following entities: agents that represent common pool resource users and the environment. The state variables characterizing these entities are listed in Table 2:

Simulations of the model do not pertain to any spatial and temporal scales but may vary across different contexts. The model runs for $T = 40000$ periods. With 1000 agents, this number of periods translates to forty generations, enough for the model to reach a steady state.

The processes that repeat every time step are the random selection of an agent, four processes concerning the selected agents' decision-making (observation, heuristic selection, expectation formation, and payoff evaluation), the updating of the average extraction level, the updating of the resource state, and the updating of all agents' perceptions of the resource state. An agent is randomly selected to act each round to approximate continuous time model behavior.

The most important design concepts of the model are objectives, prediction, and sensing. Utility maximization, which occurs according to the payoff evaluation submodel, is the main objective. It

drives agents' adaptive behavior and, in turn, the evolution of the resource. Given the computational and information constraints implied by bounded rationality, making an optimal decision requires agents to form expectations about strategic behavior in the population. This process is based on the Heuristics Switching Model [23], which offers a menu of simple rules that imply realistic computational costs. Moreover, agents with more information about the game they are playing can make better decisions. Sensing entails acquiring information on the strategic behaviors of the other players and is carried out by the observation submodel.

Key processes in the model are observation, payoff evaluation, updating the average extraction level, and updating the resource state. First, observation works as follows. Agents observe the strategic decisions of all users with whom they have a social tie. Social ties are determined by the Barabasi-Albert algorithm. Each agent i keeps track of strategic decisions using a ledger with an entry for each agent. Entries that correspond to agent j that agent i has a social tie with change whenever agent j is selected and chooses a strategy. Agents use this ledger to update their perception of the resource state and form expectations about the future. Agents update their perception of the resource state each round. They take a snapshot of their ledger whenever they act and use these snapshots to form expectations.

Second, payoff evaluation is performed by computing the utility advantage of extracting with high relative to low effort. The payoffs depend on an agent's strategy relative to the population and the resource state. Consequently, the payoff functions driving agents' adaptive behavior consider dependencies in the environmental state n_{t-1}, expectations regarding the other users' strategic decisions z_t^e, and an interaction $n_{t-1}z_t^e$:

$$\begin{aligned} \pi_t^H(n_{t-1}, z_t^e) &= \alpha + \gamma_1^H z_t^e + \gamma_2^H n_{t-1} + \gamma_3^H n_{t-1} z_t^e \\ \pi_t^L(n_{t-1}, z_t^e) &= \gamma_1^L z_t^e + \gamma_2^L n_{t-1} + \gamma_3^L n_{t-1} z_t^e \end{aligned} \tag{2}$$

The utility advantage is defined as $U_t^d = \pi_t^H - \pi_t^L$. Therefore, extracting with high effort is better when $U_t^d > 0$ and extracting with low effort when $U_t^d < 0$.

Third, updating the average extraction level uses a weighted average of all agents' actions. The weights are determined by the degrees d of all agents and the inequality of impact parameter ν:

$$W_i = \frac{d_i^\nu}{\sum_j^P d_j^\nu} \tag{3}$$

Equation 4 applies these weights to individual agents' strategies to obtain the fraction of agents extraction with low effort z_t:

$$z_t = \sum_i^P S_i W_i \tag{4}$$

Here, S_i equals 1 if agent i extracts with low effort and 0 if they extract with high effort.

Finally, the updating of the resource state is based on the current resource state and the average extraction level:

$$n_t = n_{t-1} + \frac{\epsilon}{P}(z_t - n_{t-1}) \tag{5}$$

The law of motion dictates that the resource state n_t closes a share $\frac{\epsilon}{P}$ of the gap between its current state n_{t-1} and the average extraction level z_t in every period. The parameter ϵ denotes the relative speed of environmental to strategic dynamics. This law of motion captures the qualitative dynamics of decaying and renewing resources [5].

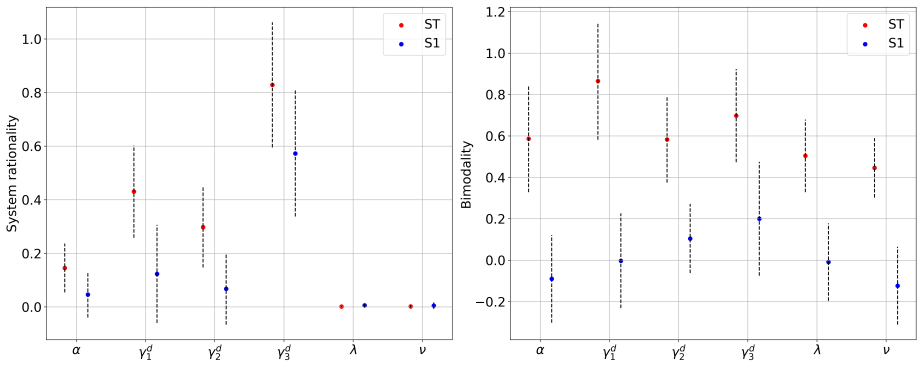

Figure 6: This plot is based on very few samples so the numbers make no sense. The first-order (blue) and total-order (red) Sobol' indices of the the paramarters α, γ_1^d, γ_2^d, γ_3^d, λ, and ν. The dots provide the estimates and the dashed lined the confidence interval of the estimates. The plot on the left is for system rationality and the plot on the right is for bimodality. Sensitivity indices indicate the shares of an output's variance attributed to a specific input factor. First-order indices offer one-factor-at-a-time sensitivities and do not consider interactions between variables. Their sum must equal unity per output. Total-order indices do consider interactions between variables. Their sum per output may exceed unity.

Global Sensitivity Analysis

This appendix presents a Sobol' sensitivity analysis to examine the influence of key input factors on the model outputs. The Sobol'-Saltelli sampling scheme [24, 25, 26] is employed.

We consider two output variables: system rationality and bimodality. Understanding the drivers of deviations from the FIE is critical. The size of these deviations can be attributed to system parameters through a measure of system rationality, described in the Appendix. This measure decreases faster the more frequent and the more significant deviations from the FIE are throughout a simulation after a burn-in of ten generations.

Second, the model may generate bistable resource outcomes. We include a measure of bimodality to identify which input variables cause these dispersed dynamics. Specifically, the sensitivity analysis incorporates the p-value of Hartigan's dip test. Hence, it does not measure the size of the difference but rather its existence. The test statistics are based on the resource state in the last period per simulation.

Discussion of the SA results.

System Rationality

Deviations from the FIE are quantifiable using a measure of system rationality, inspired by [27]. This measure compares the probabilities of high- and low-effort extraction in the REE to the probabilities observed in the boundedly rational outcome, using the Kullback-Leibler (KL) divergence [28]. The KL divergence measures the distance between the FIE probability distribution (R) and the boundedly rational outcome probability distribution (Q). Because the KL divergence is not symmetric, it is common to take the average, also known as the Jensen-Shannon divergence [29]:

$$Div(P\|Q) = \frac{\sum_i P(i) \ln \frac{R(i)}{M(i)} + \sum_i Q(i) \ln \frac{Q(i)}{M(i)}}{2} \tag{6}$$

Here, M is the distribution resulting from averaging the two probability distributions R and Q. The measure for system rationality follows from the average divergence over time:

$$System\ rationality = -\frac{1}{T}\sum_{t=1}^{T} Div(R_t \| Q_t) \tag{7}$$

The negative sign in equation 7 reflects that a more negative divergence corresponds to a lower average system rationality. This approach has the drawback that the REE is deterministic. Interpreting the fractions of players extracting with high and low effort as probabilities allows for the computation of system rationality.

Hartigan's dip test

To test for bimodality within samples of the global sensitivity analysis, we employ Hartigan's dip test [30]. It measures multimodality in a sample by the maximum difference - over all sample points - between the empirical distribution function and the unimodal distribution function that minimizes that maximum difference. The null hypothesis is that the empirical distribution function is unimodal, while the alternative is that that it is non-unimodal, i.e., at least bimodal. We use Hartigan's dip test because it makes no further assumptions about the form of the null distribution other than unimodality.

The sample size used in the global sensitivity analysis is 30. The global sensitivity analysis considers the effect of input parameters on the p-value of the statistical test. Hence, we do not employ a specific p-value as a cutoff for significance. We implemented the dip using the `diptest` package in Python.